J. Phys. Chem. A **2002,** *106,* 3181−3184 **3181**

Theoretical Study of the Reaction of Boron with Methanol and the Decomposition Paths of the Reaction Products

Suk Ping So[†]

Chemistry Department, The Chinese University of Hong Kong,
Shatin, N.T., Hong Kong, People's Republic of China

Received: September 17, 2001; In Final Form: January 11, 2002

Gaussian-2 molecular orbital calculations predict that the insertions of boron into the CH, OH and CO bonds of methanol to form $CH_2(BH)OH$, CH_3OBH, and CH_3BOH are exothermic by 56.3, 92.8, and 115.9 kcal mol^{-1}, respectively. The dissociation of CH_3OBH into CH_3 and HBO has a low activation energy of 17.6 kcal mol^{-1}. Although the loss of a methyl hydrogen from CH_3BOH has a moderate barrier (53.5 kcal mol^{-1}), the elimination of its hydroxyl hydrogen to yield CH_3BO has only a very low endothermicity (4.8 kcal mol^{-1}). CH_3BO may eventually yield the final product CH_2BO observed either by dehydrogenation with a high endothermicity of 100.2 kcal mol^{-1} or by 1,3-H shift to CH_2BOH with a high barrier of 91.7 kcal mol^{-1} and subsequent dehydrogenation. Hence, these two paths via which CH_2BO is formed are, energywise, almost equally probable.

Introduction

Laser-ablated boron atoms have been found to react with methanol.[1] The reaction products have been trapped in argon matrix and studied by FTIR spectroscopy. Isotopic substitution studies and calculations of the vibrational frequencies of the potential reaction products at the MP2/D95* level of theory have helped to identify CH_3BO, CH_2BOH, CH_2BO, and HBO as the major products. It has been proposed[1] that HBO is formed from boron insertion into the OH bond of CH_3OH and subsequent CO bond cleavage (reaction 1), while the other products are formed from boron insertion into the CO bond of CH_3OH followed by dehydrogenations only (reaction 2), or by arrangement and dehydrogenations as represented by reaction 3 because the formation of CH_2BOH directly from CH_3BOH (reaction 4) is thermodynamically less favored with respect to that of CH_3BO. However, no products resulting from boron insertion into the CH bond of CH_3OH (reaction 5) have been identified. It is thus thought desirable to carry out a high-level ab initio calculation involving more detailed characterization of transition states of the above proposed reactions 1−5.

$$CH_3OH + B \rightarrow CH_3OBH \xrightarrow{(1a)} CH_3 + HBO \tag{1}$$

$$CH_3OH + B \rightarrow CH_3BOH \xrightarrow{(2a)} CH_3BO \xrightarrow{(2b)} CH_2BO \tag{2}$$

$$\rightarrow CH_3BO \xrightarrow{(3b)} CH_2BOH \xrightarrow{(3c)} CH_2BO \tag{3}$$

$$\xrightarrow{(4a)} CH_2BOH \tag{4}$$

$$CH_3OH + B \rightarrow CH_2(BH)OH \tag{5}$$

Calculations

The structures of the various species studied were optimized by the energy gradient method at the restricted (for singlet states) and the unrestricted (for doublet states) HF/6-31G* and MP2(FU)/6-31G* levels of theory (FU denotes "full", meaning inclusion of both inner- and valence-shell electrons), using the Gaussian 98 package of programs[2] implemented on our DEC 600 AU, and COMPAQ XP900 and XP1000 workstations. Various techniques were used to determine transition state structures. Initial geometries were either guessed from the reactant and/or product structures, or located by partial geometry optimization with an appropriate bond held at a series of fixed values. These initial geometries were then fully optimized, i.e., all geometrical parameters allowed to change in value, using the automated TS option of Gaussian 98. When the initial symmetry of a species (equilibrium or transition state structure) changed to a practically higher one on geometry optimization, its geometry was then reoptimized under the constraint of the latter symmetry. For example, geometry optimization under C_1 symmetry yielded a nearly C_s structure for the insertion products CH_3BOH, CH_3OBH, and $CH_2(BH)OH$. Hence, they were reoptimized with a C_s symmetry constraint imposed.

The energies of the optimized structures were computed at the Gaussian-2 (G2) theory,[3] which is the improved Gaussian-1 (G1) theory.[4,5] The conventional G2 method uses a series of frozen-core (FC) QCISDT, MP4SDTQ, and MP2 single-point energy calculations on the MP2(FU)/6-31G* structures with various basis sets to approximate a full QCISDT(FC)/6-311+G(3df,2p)//MP2(FU)/6-31G* calculation, incorporating a so-called "higher order correction" based on the number of paired and unpaired electrons and scaled HF/6-31G* zero-point vibrational energies (ZPEs). However, in the present work, MP2(FU)/6-31G* zero-point vibrational energies scaled by a factor of 0.9427 were used.[6] In addition, the G2Q method[7] was modified (see below) and used for the calculation of G2 energies of some doublet transition state structures whose calculated $\langle S^2 \rangle$ values deviate appreciably from the value of 0.75 for a pure doublet state (see below).

Vibrational frequencies were determined by the analytical evaluation of the second derivatives of energy to verify the nature (equilibrium or transition state) of the stationary point

---

[†] Fax: +852-2603-5057. E-mail: sukpingso@cuhk.edu.hk.

10.1021/jp013557p CCC: \$22.00

structures optimized, to provide zero-point vibrational energy corrections, and to predict vibrational frequencies of the stable species for the sake of their identification by infrared spectroscopy.

The connection between a transition state structure and its reactants and products was established, at the MP2(FU)/6-31G* level of theory, by the intrinsic reaction coordinate (IRC) calculations based on the reaction path following the algorithm of Gonzalez and Schlegel[8,9] as coded in Gaussian 98, or by optimization starting from a transition state structure with one or two of its geometrical parameters distorted.

Results and Discussion

The various stationary point structures studied are depicted in Figure 1 together with their optimized geometrical parameters. The calculated structures have been shown to be either equilibrium structures (**1**−**9**) or transition state structures (**TS1a**, **TS3b**, **TS3c**, and **TS4a**) by their HF/6-31G* and MP2(FU)/6-31G* vibrational frequencies. Structures **TS1a**, **TS3b**, **TS3c**, and **TS4a** are the transition state structures for the decomposition of CH_3OBH to CH_3 + HBO (reaction step 1a), the 1,3-H shift reaction of CH_3BO (reaction step 3b), and H-eliminations of CH_2BOH and CH_3BOH (reaction steps 3c and 4a), respectively. Table 1 lists the scaled MP2(FU)/6-31G* harmonic vibrational frequencies of the stable boron-containing species studied together with experimental values available.[1] Since the observed frequencies are for bands of the species in argon matrix, the agreement between the predicted and the observed frequencies is considered to be reasonable.

It is noted from Figure 1 that the inclusion of electron correlation up to the MP2 level in geometry optimization gives the expected small changes in bond lengths and bond angles (~0.05 Å and ~5° or less) for the equilibrium structures **1**−**9**. However, some of the geometric parameters of the transition state structures undergo changes as large as about 0.14−3.24 Å and 8°−66.5° (Figure 1). This shows that electron correlation is very important for transition state structures. Hence, MP2(FU)/6-31G* zero-point vibrational energies scaled by a factor[6] of 0.9427 were used instead in the calculation of the G2 energies.

It is interesting to note from Figure 1 that, at the MP2(FU)/6-31G* level, the geometric parameters of the CH_3OH subunit not directly involved in the insertion reaction undergo only a very small change in value (0.019 Å and 4.7° or less) in the formation of the insertion products CH_3OBH and $CH_2(BH)OH$. The calculated XBY (X, Y = H, C, O) bond angle lies between 120.0° and 124.7° for the three insertion products CH_3OBH, CH_3BOH, and $CH_2(BH)OH$, but is 180° for the other equilibrium structures CH_3BO, CH_2BOH, CH_2BO, and HBO. This shows that the boron atom in the former three and the latter four structures has sp^2 and sp hybridized bonding orbitals, respectively. Comparison of the calculated BH, BC, and BO bond lengths with the sums of the corresponding atomic radii[10] (single/double/triple bond radius: H = 0.30/−/−, B = 0.81/0.71/0.64, C = 0.77/0.67/0.60, and O = 0.74/0.62/0.55 Å) and the corresponding experimental bond distances in some boron compounds[11] (e.g., BH = 1.23 Å for BH, *t*-BH = 1.19 Å for B_2H_6, BC = 1.56 Å for $B(CH_3)_3$, BO = 1.38 Å for $B(OCH_3)_3$ and 1.36 Å for $B(OH)_3$, and BO = 1.20 Å for BO) leads to the following observations:

(1) The BH bonds (1.171−1.197 Å) of CH_3OBH, $CH_2(BH)OH$, and HBO are single bonds.

(2) The BC bonds (1.508−1.567 Å) of CH_3BOH, $CH_2(BH)OH$, CH_3BO, and CH_2BO are single bonds, but that (1.390 Å) of CH_2BOH has some double bond character.

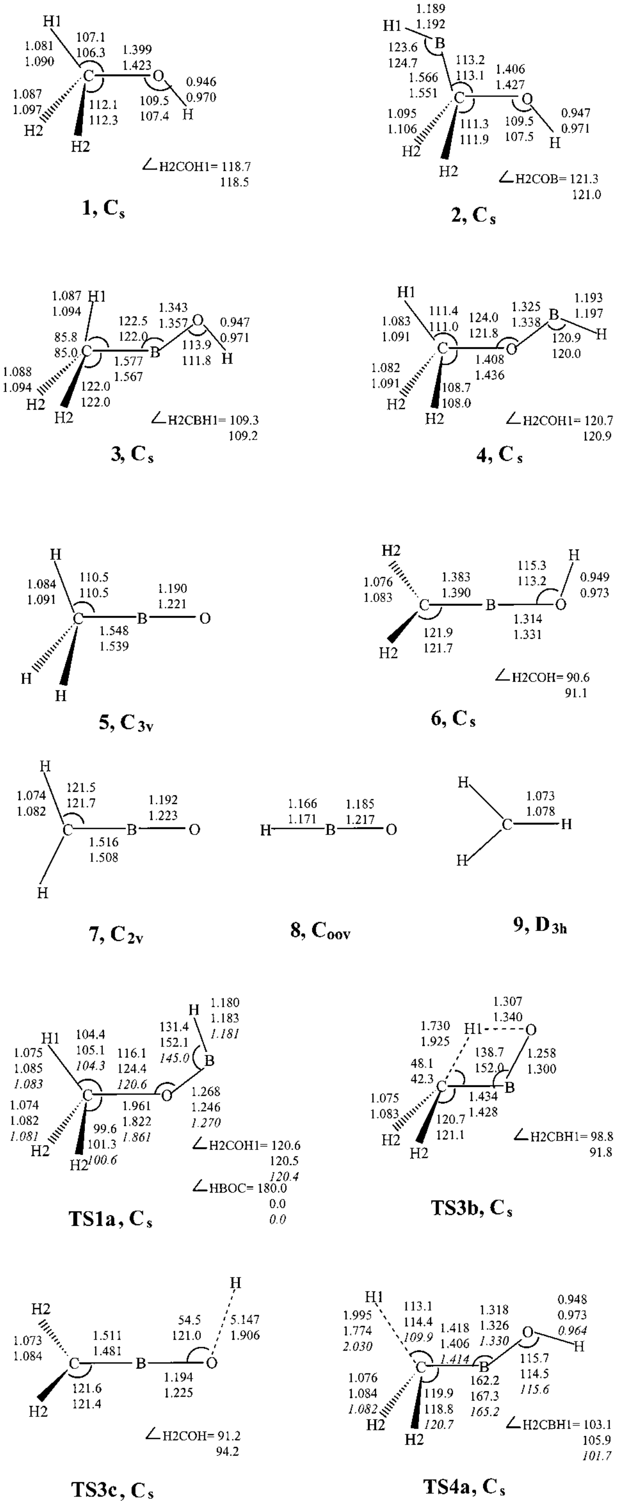

Figure 1. Optimized structures of species studied. Bond lengths are in angstroms and angles in degrees. HF/6-31G* values are shown above the MP2(FU)/6-31G* ones, and QCISD/6-31+G(d,p) values are in italics.

(3) The BO bonds of CH_3OBH, CH_3BOH, and CH_2BOH (1.331−1.357 Å) are double bonds, but those of CH_3BO, CH_2BO, and HBO (1.217−1.223 Å) are shorter still.

A boron atom has the electronic configuration $1s^22s^22p^1$ and a maximum valence of 3. Hence, the unexpectedly short BC bond of CH_2BOH (shorter than a single bond) and BO bonds of CH_3BO, CH_2BO, and HBO (shorter than a double bond) may be attributed to the overlapping of the filled nonbonding $p\pi$ orbital of the C or O atom with the vacant $p\pi$ orbital of the B

TABLE 1: MP2(FU)/6-31G* Harmonic Vibrational Frequencies[a] of the Stable B-Containing Species Studied

species	frequencies (cm^{-1})
CH_3OBH	129, 362, 517, 883, 1014, 1142, 1149, 1335, 1454, 1470, 1479, 2529, 2942, 3041, 3045
CH_3BOH	40, 352, 544, 792, 826, 871, 1086, 1280, 1336, 1436, 1445, 2922, 3010, 3012, 3580
$CH_2(BH)OH$	315, 369, 404, 553, 738, 940, 1058, 1171, 1172, 1367, 1427, 2582, 2830, 2865, 3556
CH_3BO	340, 340, 783, 902(895.6),[b] 902(896.8), 1327, 1442 (1305.0), 1442 (1305.0), 1900 (1972.4), 2950, 3040, 3040
CH_2BOH	309, 333, 597, 612, 770, 892, 971, 1337, 1724 (1748.3), 3053, 3134, 3556
CH_2BO	336, 377, 601 (663.6), 847, 871, 1403, 1903 (1946.6), 3070, 3167
HBO	734 (756.7), 734 (756.7), 1725 (1821.9), 2808

[a] Frequencies have been uniformly scaled by a factor of 0.9427. [b] Frequencies of observed IR bands for species in argon matrix from ref 1 are in parentheses.

atom. The ionic−covalent resonance of the bond and the incomplete octet of the B atom have also been considered[12] to be additional factors for the shortness of the BX (X = O, F, Cl, Br) bonds in BR_3 compounds.

The $\langle S^2 \rangle$ values of doublet structures obtained from unrestricted HF/MP2 wave functions are 0.754/0.754 for B, 0.753/0.753 for the insertion products, 0.765/0.767 for CH_2BO, and 0.761/0.762 for CH_3. These are almost identical with the value of 0.75 of a pure doublet state. Hence, for these species, the unpredictable spin contamination effect due to unrestricted wave functions on molecular geometry[13] may be neglected. However, the respective $\langle S^2 \rangle$ values of **TS1a** and **TS4a** are 1.091/0.908 and 0.895/0.886, which deviate appreciably from 0.75.

For 13 test reactions of small open-shell systems (including a $^3\Pi$ and an $^2A'$ transition state with SCF $\langle S^2 \rangle$ values of 3.05 and 2.32, respectively), Durant et al.[7] have found that the standard G2 method yields classical barrier heights in reasonable agreement (with an absolute average deviation of 1.5 kcal mol^{-1}) with the results of CASSCF/MRCI calculations and experiment, and its performance is improved by the use of QCISD/6-311G(d,p) geometries and frequencies only for the transition states involved (known as the G2Q method).[7] Henceforth, several modified G2 methods have been proposed[14] for the study of highly spin-contaminated systems, but there is no consensus as to which of them will give the most reliable results. Recently, Chung et al.[15] carried out various UHF, UMP2, ROMP2, UMP4, QCI, and CC calculations on four test hydrogen abstraction reactions whose transition states have spin contamination in the range of 0.754−0.970. They concluded that for geometries of open-shell transition states the correlated treatment which goes beyond second-order excitation is more important than that which eliminates spin contamination, and recommended the latter two methods for open-shell transition state structures with significant spin contamination. Hence, the G2Q method[7] is chosen for the reinvestigation of **TS1a** and **TS4a**. However, because of some long bonds obtained for these structures at the MP2(FU/6-31G* level, the addition of diffuse functions may be preferable. Accordingly, the G2Q method is modified (denoted as G2Q(D)) to use QCISD/6-31+G(d,p) geometries and frequencies scaled by 0.9538 (a scaling factor recommended[6] for QCISD/6-31G(d) frequenceis), and 6-311+G(d,p) and 6-311+G(2df,p) functions in place of 6-311G(d,p) and 6-311G(2df,p) ones for single point energy calculations of the original G2 method. Table 2 collects the G2 energies of the species studied from which relative energies between various structures can be easily deduced.

The insertion reactions of boron into the OH, CO, and CH bonds of methanol have been computed to form the products CH_3OBH, CH_3BOH, and $CH_2(BH)OH$ of C_s symmetry. The transition state structures of these reactions have been searched for at the MP2(FU)/6-31G* level, but, unfortunately, could not be characterized. Thus, no definite conclusions on the barriers of these insertion reactions can be made. The insertion products CH_3OBH, CH_3BOH, and $CH_2(BH)OH$ are predicted to be lower in energy than the reactants ($CH_3OH + B$) by 92.8, 115.9, and 56.3 kcal mol^{-1} at the G2 level (87, 107, and 49 kcal mol^{-1} at the MP2/D95* level[1]), respectively. Hence, the insertion reactions studied are exothermic, the CH bond insertion being the thermodynamically least favored one.

TABLE 2: G2 Total Energies of Species Studied

species	energy (hartrees)
CH_3OH	−115.534 698
CH_3OBH	−140.284 644
CH_3BOH	−140.321 438
$CH_2(BH)OH$	−140.226 532
CH_3BO	−139.813 718
CH_2BOH	−139.741 329
CH_2BO	−139.154 089
HBO	−100.566 501
CH_3	−39.743 946
B	−24.602 036
H	−0.500 000
TS1a	−140.256 562[a]
TS3b	−139.667 588
TS3c	−139.659 167
TS4a	−140.236 118[a]

[a] G2Q(D) values (see text)

The other products BH, BCO, and CH_2O which have also been observed[1] may be formed potentially from the CH bond insertion product $CH_2(BH)OH$. However, alternatively, under the reported experimental condition,[1] H, CO, and CH_2O can be produced photolytically from CH_3CO and thus BH and BCO generated by the reaction of H and CO with boron. Hence, in view of the above results and the strongness of the bond, the CH bond insertion reaction may be considered relatively unimportant and is neglected in the boron−methanol reaction.

The dissociation of the OH bond insertion product CH_3OBH into CH_3 and HBO (reaction step 1a) has been found to be exothermic by 16.2 kcal mol^{-1} at the G2 level and proceed via a transition state structure **TS1a** with an activation barrier of 17.6 kcal mol^{-1}. It is seen from Figure 1 that the CH, BO, and BH bond lengths of **TS1a** are much closer to the corresponding bond lengths of the dissociation products CH_3 and HBO than those of the reactant CH_3OBH. Hence, **TS1a** is a late transition state structure.

The CO bond insertion product CH_3BOH may be converted to CH_3BO or CH_2BOH by elimination of the hydroxyl hydrogen (reaction step 2a) or a methyl hydrogen (reaction step 4a), respectively. The present work shows that reaction 2a is an endothermic reaction with no activation barrier while reaction 4a occurs via a transition state structure **TS4a**. It is significant to find that the activation barrier (53.5 kcal mol^{-1}) of reaction 4a is not only moderately large but, more importantly, also more than 10 times larger than the endothermicity (4.8 kcal mol^{-1}) of reaction 2a. In addition, reaction 4a is endothermic by 50.3 kcal mol^{-1}. Thus, reaction 4a is much less favored, not only thermodynamically as noted by Lanzisera et al.,[1] but also kinetically in terms of activation energy. Geometric data shown in Figure 1 indicate **TS4a** to also be a late transition state structure.

The dissociation product CH_3BO may yield the final product CH_2BO either by dehydrogenation only (reaction step 2b) or by isomerization via a 1,3-H shift to CH_2BOH (reaction step 3b), which then loses a hydroxyl hydrogen to become CH_2BO (reaction step 3c). Reaction 2b, like reaction 2a, is predicted to occur with no activation barrier but an endothermicity of 100.2 kcal mol^{-1} at the G2 level, while the isomerization 3b goes through a transition state structure **TS3b** with a barrier of 91.7 kcal mol^{-1}. Hence, energywise, reaction 3b is only slightly favored over reaction 2b. The conversion of CH_2BOH to CH_2BO is found (Table 2) to occur via a transition state **TS3c** (most likely an artifact; see below) with an activation energy of 51.6 kcal mol^{-1}, and to have an endothermicity of 54.7 kcal mol^{-1} As a result, the rate-determining steps of reactions 2 and 3 in the generation of CH_2BO are 2b and 3b, respectively.

Reaction 3c is predicted above to have, unexpectedly, an activation energy smaller than its endothermicity by 3.2 kcal mol^{-1} at the G2 level; i.e., the energy ($-139.659\,167$ hartrees) of the transition state structure **TS3c** is lower than the sum ($-139.654\,089$ hartrees) of the energies of the decomposition products CH_2BO and H, even though **TS3c** has been shown by IRC calculations to connect to CH_2BOH and these products. However, data in Figure 1 show that **TS3c** is a late transition state structure with geometric parameters very much closer to those of the product CH_2BO than those of the reactant CH_2BOH. In addition, though the value of 3.2 kcal mol^{-1} greatly differs from the average absolute deviation of 1.21 kcal mol^{-1} of the G2 method from experiment,[16] it should not be overemphasized. Hence, it is not too unreasonable to conclude that **TS3c** is most likely an artifact rather than an actual transition state, and the dehydrogenation of CH_2BOH to CH_2BO (reaction 3c) has no barrier but an endothermicity of 54.7 kcal mol^{-1}.

As noted above, the CB and the BO bonds of CH_3BOH, CH_3BO, CH_2BOH, and CH_2BO are respectively single and double, single and partially triple, double and double, and single and partially triple bonds. Hence, in terms of π-bond or electron delocalization effect, the product CH_2BO of the hydroxyl hydrogen elimination reaction 3c is less stabilized or even destabilized over its reactant CH_2BOH in comparison with the stabilization of CH_3BO over CH_3BOH of reaction 2a. This may attribute, partly at least, to the above prediction of this work that reaction 2a has a much smaller endothermicity than reaction 3c.

Acknowledgment. The author thanks his department for a financial allocation and his university for a Special Equipment Grant to support the acquisition of the workstations.

References and Notes

(1) Lanzisera, D. V.; Andrews, L. *J. Phys. Chem. A* **1997**, *101*, 1482.

(2) Frisch, M. J.; Trucks, G. W.; Schlegel, H. B.; Scuseria, G. E.; Robb, M. A.; Cheeseman, J. R.; Zakrzewski, V. G.; Montgomery, J. A., Jr.; Stratmann, R. E.; Burant, J. C.; Dapprich, S.; Millam, J. M.; Daniels, A. D.; Kudin, K. N.; Strain, M. C.; Farkas, O.; Tomasi, J.; Barone, V.; Cossi, M.; Cammi, R.; Mennucci, B.; Pomelli, C.; Adamo, C.; Clifford, S.; Ochterski, J.; Petersson, G. A.; Ayala, P. Y.; Cui, Q.; Morokuma, K.; Malick, D. K.; Rabuck, A. D.; Raghavachari, K.; Foresman, J. B.; Cioslowski, J.; Ortiz, J. V.; Stefanov, B. B.; Liu, G.; Liashenko, A.; Piskorz, P.; Komaromi, I.; Gomperts, R.; Martin, R. L.; Fox, D. J.; Keith, T.; Al-Laham, M. A.; Peng, C. Y.; Nanayakkara, A.; Gonzalez, C.; Challacombe, M.; Gill, P. M. W.; Johnson, B. G.; Chen, W.; Wong, M. W.; Andres, J. L.; Head-Gordon, M.; Replogle, E. S.; Pople, J. A. *Gaussian 98*, revision A.7; Gaussian, Inc.: Pittsburgh, PA, 1998.

(3) Curtiss, L. A.; Raghavachari, K.; Trucks, G. W.; Pople, J. A. *J. Chem. Phys.* **1991**, *94*, 7221.

(4) Pople, J. A.; Head-Gordon, M.; Fox, D. J.; Raghavachari, K.; Curtiss, L. A. *J. Chem. Phys.* **1989**, *90*, 5622.

(5) Curtiss, L. A.; Jones, C.; Trucks, G. W.; Raghavachari, K.; Pople, J. A. *J. Chem. Phys*. **1990**, *93*, 2357.

(6) Scott, A. P.; Radom, L. *J. Phys. Chem.* **1996**, *100*, 16502.

(7) Durant, J. L., Jr.; Rohlfing, C. M. *J. Chem. Phys.* **1993**, *98*, 8031.

(8) Gonzalez, C.; Schlegel, H. B. *J. Chem. Phys.* **1989**, *90,* 2154.

(9) Gonzalez, C.; Schlegel, H. B. *J. Chem. Phys.* **1990**, *94,* 5523.

(10) Pauling, L. *The Nature of the Chemical Bond*, 3rd ed.; Cornell University Press: Ithaca, NY, 1960

(11) Gray, H. B. *Electrons and Chemical Bonding*; W. A. Benjamin, Inc.: New York, 1965, and references therein.

(12) Cotton, F. A.; Wilkinson, G. *Advanced Inorganic Chemistry*, 3rd ed.; Interscience Publishers: New York, 1972.

(13) Kutzelnigg, W. *Angew. Chem., Int. Ed. Engl.* **1984**, *23*, 272.

(14) Mebel, A. M.; Morokuma, K.; Lin, M. C. *J. Phys. Chem.* **1995**, *99*, 7414, and references therein.

(15) Chung, Y. Y.; Coitino, E. L.; Truhlar, D. G. *J. Phys. Chem. A* **2000**, *104*, 446.

(16) Curtiss, L. A.; Carpenter, J. E.; Raghavachari, K.; Pople, J. A. *J. Chem. Phys.* **1992**, *96*, 9030.